Published in final edited form as:
*Magn Reson Med*. 2008 May ; 59(5): 1021–1029. doi:10.1002/mrm.21524.

# Resting-State Functional Connectivity of the Rat Brain

**Christopher P. Pawela**[1], **Bharat B. Biswal**[2], **Younghoon R. Cho**[3], **Dennis S. Kao**[3], **Rupeng Li**[1], **Seth R. Jones**[3], **Marie L. Schulte**[4], **Hani S. Matloub**[3], **Anthony G. Hudetz**[4], and **James S. Hyde**[1,*]

1*Department of Biophysics, Medical College of Wisconsin, Milwaukee, Wisconsin, USA*

2*Department of Radiology, University of Medicine and Dentistry of New Jersey (UMDNJ), New Jersey Medical School, Newark, New Jersey, USA*

3*Department of Plastic Surgery, Medical College of Wisconsin, Milwaukee, Wisconsin, USA*

4*Department of Anesthesiology, Medical College of Wisconsin, Milwaukee, Wisconsin, USA*

## Abstract

Regional-specific average time courses of spontaneous fluctuations in blood oxygen level dependent (BOLD) MRI contrast at 9.4T in lightly anesthetized resting rat brain are formed, and correlation coefficients between time course pairs are interpreted as measures of connectivity. A hierarchy of regional pairwise correlation coefficients (RPCCs) is observed, with the highest values found in the thalamus and cortex, both intra- and interhemisphere, and lower values between cortex and thalamus. Independent sensory networks are distinguished by two methods: data driven, where task activation defines regions of interest (ROI), and hypothesis driven, where regions are defined by the rat histological atlas. Success in these studies is attributed in part to the use of medetomidine hydrochloride (Domitor) for anesthesia. Consistent results in two different rat-brain systems, the sensorimotor and visual, strongly support the hypothesis that resting-state BOLD fluctuations are conserved across mammalian species and can be used to map brain systems.

### Keywords

BOLD resting-state signal; rat fMRI; visual system; sensorimotor system

---

Functional connectivity in the resting human brain using blood oxygen level dependent (BOLD) contrast is revealed by analysis of a series of MRI echo planar images acquired over a period of several minutes with the subject at rest (1). In the present work, functional connectivity experiments are extended from human brain to rat brain and our central hypothesis is that the underlying physiology is conserved across all mammalian species.

A reference time course obtained from a reference voxel (or, alternatively, an average over a cluster of voxel time courses in a region of interest [ROI]) is formed. Cross correlation of the reference time course with all voxel time courses in the slice provides a functional connectivity map. A strategy is required for selection of the reference time course, and performance of a task is commonly used to define ROIs in resting brain that can be used to form reference time courses.

*Correspondence to: James S. Hyde, Ph.D., Department of Biophysics, Medical College of Wisconsin, 8701 Watertown Plank Road, Milwaukee, WI 53226. E-mail: jshyde@mcw.edu

We have discovered that electrical stimulation using an implanted electrode on the radial nerve of the brachial plexus of a rat (2) results in activation of a network of sensorimotor brain regions, each of which is a suitable candidate for formation of a reference time course when analyzing resting-state data. Experiments not only in the sensorimotor system but also in the visual system provide further support for our central hypothesis. Functional connectivity was studied using reference waveforms obtained from areas that were found to be activated by light incident on the retina that was turned on and off in a block-trial functional MRI (fMRI) experiment.

Anatomic images acquired in this experiment are of high quality, and it is possible to define anatomic regions purely by reference to the rat histological atlas (3). One can develop a reference waveform from each of these regions and test a specific hypothesis that functional connectivity to a second region is consistent with a known connectivity. We report here success in this hypothesis-driven approach to analysis of resting-state data. A total of 22 sensorimotor regions were identified, and connectivities between each of these regions and the other 21 regions were determined.

Most functional connectivity studies have been in the awake human brain (1,4). Lowe et al. (5) extended our early results by demonstrating correlations over larger regions of the sensorimotor cortex. Xiong et al. (6,7) established relationships between the motor and association cortices. They observed resting-state correlation relationships between these motor and association areas, specifically the anterior and posterior cingulate cortical regions known to be involved in attention. Subsequently, Hampson et al. (8) demonstrated the presence of resting-state connectivity in sensory cortices, specifically in the auditory and visual domains. Hampson et al. (9) and Greicius et al. (10) observed resting-state correlations in the anterior and posterior cingulate areas. Activation during a visual attention task indicated similar cingulate activity (9,10). Vincent et al. (11) recently reported connectivity patterns in anesthetized monkey brain and concluded that the underlying phenomenon of spontaneous oscillations in blood oxygenation is conserved in primate brain.

Figure 1a shows a simplified flowchart displaying the brain-system connections involved in the motor and sensory networks in the rodent brain as defined by prior histological studies (12,13). Regions listed in the cortex include the primary/secondary motor areas (M1/M2) and primary/secondary sensory areas (S1, S2). The corpus callosum (CC) contains the highest number of connections to the cortex. The sensorimotor thalamus (SMT) includes the ventral posterior medial thalamic nucleus/ventral posterior lateral thalamic nucleus (VP), the posterior thalamic nucleus (PO), and the ventral lateral thalamic nucleus (VL). The caudate putamen (CP) and globus pallidus (GP) are included as parts of the basal ganglia.

Figure 1b is a simplified flowchart displaying the two main pathways involved in the rodent visual network as defined by prior anatomical tract tracing studies (12,13). One pathway works into the cortex through the thalamic dorsal lateral geniculate nucleus (DLG) and the other through the superior colliculus (SC) into the lateral posterior thalamic nucleus (LP). The cortex includes the primary and secondary visual areas (V1/V2) and association cortex (TeA). As in the motor system, the functional anatomy from the visual system was used to define reference voxels for subsequent resting-state analysis. Regions within the networks of Fig. 1a and b were used to generate regional pairwise correlation coefficient (RPCC) matrices in our hypothesis-driven method.

## MATERIALS AND METHODS

### Animal Usage

A total of 25 Sprague Dawley rats ($N = 25$) (Charles River Laboratories, Wilmington, MA, USA) weighing 300-450 g were used for this study. A total of five rats ($N = 5$) were used for

the BOLD fMRI experiments on the radial nerve of the rat upper extremity. A total of five rats ($N = 5$) were used in the experiments on the BOLD fMRI signal of the rat visual system. A total of 15 unbiased rats ($N = 15$) were used for study of the BOLD physiological fluctuations in the resting-state signal. All animals were used in accordance with the policies and procedures of the Medical College of Wisconsin's Institutional Animal Care and Use Committee.

### General Animal Preparation

All rats were initially anesthetized with 2% isoflurane and placed supine on a heated surgical table. Isoflurane was maintained at 1.2% to 1.5%. All rats then underwent a standard surgical procedure in preparation for the MRI protocol. The left femoral vein and artery were cannulated for drug infusion and blood pressure observation, respectively. A tracheostomy was performed for mechanical ventilation.

### Electrode Implantation for Radial Nerve Experiments

The five rats included in the radial nerve experiments underwent an additional procedure to isolate and attach an electrode to the radial nerve. The radial nerve, one of four major nerves supplying the upper extremity, lies deep to the pectoralis muscle and the plexus of the median and ulnar nerves. Exposure of this area required an incision along the medial aspect of the upper extremity to the axilla and onto a portion of the flank. The pectoralis muscle was exposed with careful blunt dissection and retraction of subcutaneous tissues with the aid of 7-0 prolene sutures. Medial retraction of the pectoralis muscle revealed the median, ulnar, and radial nerves along with the brachial artery. Along the lateral aspect of this neurovascular bundle lie the long and short heads of the biceps brachii muscles. To allow greater exposure of the nerves, the long head of the biceps brachii was reflected laterally with a 7-0 prolene suture. The radial nerve was identified and carefully dissected out circumferentially, manipulating the nerve solely by its epineurium. A plastic sheet was used to isolate the radial nerve. An electrode was placed around the radial nerve. A total of two small silicone sheets, one proximal and one distal, were secured to the electrode and the surrounding tissue to stabilize it and to avoid inadvertent displacement of the electrode. A final check was done to ensure the electrode contacted the radial nerve alone.

### Physiological Monitoring During fMRI Protocol

During fMRI, the blood oxygen saturation (pulse oximeter 8600V; Nonin Medical, Plymouth, MN, USA), inspired/expired $O_2$ and $CO_2$ (POET IQ2; Criticare Systems, Waukesha, WI, USA), temperature, and respiratory rate (Model 1025; SA Instruments, Stony Brook, NY, USA) of all rats were continually monitored and recorded. Invasive blood pressure was monitored through access from the femoral artery (Model 1025; SA Instruments). All physiological data were recorded in a personal computer (WinDaq Pro; DataQ Instruments, Akron, OH, USA). Arterial blood gases were sampled hourly (i-Stat; Helska, Loveland, CO, USA). All physiological parameters were maintained within normal ranges.

### fMRI Protocol and General Resting-State Acquisitions

All experiments were carried out on a Bruker 9.4T (AVANCE; Bruker, Billerica, MA, USA) scanner with a 30-cm bore. After transferring the rat to the MRI scanner, an intravenous (i.v.) infusion of 0.1 mg/kg/h Domitor (medetomidine hydrochloride; Pfizer Animal Health, New York, NY, USA) and 2 mg/kg/h pancuronium bromide (Hospira, Inc., Lake Forest, IL, USA) was begun as the isoflurane was tapered to zero. The rat was loaded onto a custom-built MR imaging cradle constructed primarily from G-10 fiberglass, which has a susceptibility similar to air. The rat was maintained at 37°C by a conductive warming and cooling system that circulates water beneath the surface of the cradle (Meditherm-III; Gaymar Industries, Orchard Park, NY, USA). All rats were mechanically ventilated by an MRI compatible ventilator

(MRI-1 Ventilator; CWE, Ardmore, PA, USA) at a rate of 55-65 intakes per min, adjusted to maintain arterial blood gases within physiological limits. Images were acquired with a Bruker receive surface coil and a linear transmit coil. An initial RARE anatomical scan was acquired with a 256 × 256 matrix, TE = 50.8 ms, FOV = 35 mm, 15 slices, and 1-mm slice thickness. The 12th slice was located directly over the anterior commissure, which is centered - 0.36 from bregma. Echo-planar imaging (EPI) parameters were as follows: 96 × 96 matrix, TR = 2 s,TE = 18.76 ms, FOV = 35 mm, 15 slices, 1-mm slice thickness, and 110 time repetitions. The EPI volumes were zero-filled to 128 × 128 matrix. The slices were oriented with the same geometry as the RARE image. Total acquisition time was 3 min and 40 s. All animal subjects underwent two initial "restingstate" EPI scans prior to any stimulation protocol. Additionally, ambient lights were turned off during all image acquisitions, both "resting state" and stimulation, to prevent visual background interference.

## Specific Experimental Protocols

**Forepaw—**Following resting-state scans, all rats underwent a standard forepaw experiment as a control. Bipolar beryllium copper needles were inserted between the webspaces of digits two and four of the left forepaw. A standard block design stimulation protocol of 40 s of rest followed by stimulation for 20 s repeated for three blocks with a 40 s rest period at the end for a total of 3 min and 40 s was used. All stimulations were computer controlled and triggered by an initial pulse from the scanner. Forepaw stimulation consisted of 2-mA pulses with a pulse width of 3 ms and a frequency of 10 Hz, produced by a square pulse generator connected to a constant current unit (S88; Grass Telefactor, Warrick, RI, USA). It was verified by physiological measurements that this stimulation sequence was not painful. Two "resting-state" scans followed the forepaw stimulation in order to assess any stimulation-induced changes in the BOLD physiological fluctuation signal.

**Resting State—**The 15 rats used for the resting-state analysis underwent no further experimentation to prevent bias toward correlation between activated regions. The technique used in the resting-state analysis is described below.

**Nerve Stimulation—**In the five rats with the electrode attached to the radial nerve, the radial nerve was stimulated at 1 mA, with a pulse width and a frequency of 10 Hz. It was verified by physiological measurements that this stimulation sequence was not painful. The stimulation block design was the same as described for the forepaw control. Due to electrode implantation, these rats were excluded from the resting-state analysis. A total of two EPI acquisitions (10 total) with a time of 3 min and 40 s each were acquired and used in subsequent analysis.

**Light Stimulation—**Two blue light-emitting diodes (LEDs) with a wavelength of 465 nm were placed bilaterally, 2 cm from each eye of five rats. The LEDs were flashed with square transistor-transistor logic (TTL) pulses at a frequency of 1 Hz and a pulse width of 5 ms, using the same block design as the forepaw control experiment. Two EPI acquisitions (10 total) with a time of 3 min and 40 s each were acquired and used in subsequent analysis.

## Functional Data Analysis (Light and Nerve Stimulation)

The 10 EPI acquisitions from both the light and nerve experiments were registered to an "ideal" rapid acquisition with relaxation enhancement (RARE) anatomy using the program FLIRT (14). The "ideal" anatomy was selected by the researchers on the basis of exhibiting the highest gray/white matter contrast. After registration, the 10 registered EPI volumes from either condition were averaged using the 3dcalc program from the AFNI software suite (15). These averaged EPI data sets were used to create activation maps by performing an F-test on the time series data using the design block as the only regressor (AFNI, 3dDeconvolve). A *P* value of

0.005 was used for plotting and was the threshold considered for activation. All activation maps were overlaid on the "ideal" RARE anatomy used in the registration process.

### ROI Delineation

Brain regions were drawn freehand on the "ideal" RARE anatomy using AFNI by consultation with the Paxinos rat brain atlas (3). Regions were chosen to test for functional connectivity in the sensorimotor and visual system.

### Resting-State Data Analysis

A total of 15 separate rats, different than the 10 used in the light and radial nerve experiments, were used in the analysis of the resting state. In order to keep all subjects correctly aligned for proper ROI analysis, these data were registered to the same "ideal" RARE anatomy used in the nerve stimulation and light experiments with the program FLIRT. Only initial unbiased "resting-state" scans were used in this analysis. A low-pass filter with a cutoff at 0.1 Hz was applied to all voxel time courses on a voxel-by-voxel basis covering the entire brain (16).

**Temporal Correlation—**We used cross-correlation analysis between average time courses of six reference voxels at the center of the region chosen from the functional anatomy and those time courses were correlated with every other voxel time courses in that slice. Since we are only interested in the temporal correlation due to slow periodic spontaneous oscillations, a finite impulse response filter (16) was used to filter the high-frequency components from each of the data sets (as described above). Because of the short data size, filter parameters were adjusted to minimize the generation of artifactual frequencies (sidelobes). The correlation coefficient was then calculated using the formula

$$r = \sum \left(X_i - \bar{X}\right)\left(Y_i - \bar{Y}\right) / \sqrt{\sum \left(X_i - \bar{X}\right)^2 \sum \left(Y_i - \bar{Y}\right)^2},$$

where $X_i$ and $Y_i$ represent the *i*th time point from two voxels, and $\bar{X}$ and $\bar{Y}$ represent the means. All voxels that passed a correlation coefficient threshold of 0.35 were considered significant and locations were noted. The average across 15 rats was plotted.

**RPCC Method—**The principal component analysis (PCA) was computed (17) for each subregion within the sensorimotor or visual systems. Using PCA, a set of orthogonal data sets was determined from their energy content. Briefly, PCA is a multivariate technique that replaces the measured variables by a new set of uncorrelated variables (principal components), arranged in the order of decreasing standard deviation (SD) or energy distribution. For this study, the first two components accounted for more than 75% of the SD for each ROI and were therefore used. The resulting time series (consisting of the first PCA) for each subregion was correlated with every other time component to obtain a pair-wise correlation matrix. The average across 15 rats was tabulated. The PCA was run independently for each region.

**Statistical Significance—**A binomial sign test was used to determine the significance for the number of rats used. Assuming that there was fluctuation and connectivity or no fluctuation and no connectivity, we assigned each a probability of 0.5. For five rats, the *P* value was 0.03, and for 10 rats, the *P* value was 0.001. We felt that this was significant and chose to use 15 rats in the analysis.

## RESULTS

A BOLD resting-state voxel time course for an anesthetized rat is plotted in Fig. 1c, and the corresponding filtered power spectrum is plotted in Fig. 1d. A low-pass filter with a cutoff at 0.1 Hz was applied to all voxel time courses on a voxel-by-voxel basis covering the entire

brain. Correlations between an average time course from a six-voxel reference region and the rest of the brain were the basis for our data-driven method for resting-state analysis.

Figure 2a displays the BOLD activation pattern after stimulation of the right radial nerve ($N$ = 5). This slice is centered -3.36 mm from bregma and has a thickness of 1 mm. Several regions undergo a positive change in the BOLD signal during task activation, including the contralateral S1Tr (primary sensory trunk region), contralateral M1/M2, contralateral S2, and ipsi-/contralateral SMT. The CP undergoes a negative task activation change in the BOLD signal on both the left and right sides.

We chose reference voxels located in the center of the regions associated with sensorimotor system activation, and correlated the average filtered reference voxel time courses in a selected region with the remaining voxels in that slice. Voxels were selected based on the functional anatomy determined during direct upper forelimb nerve stimulation experiments. Analysis was performed in the same slice as Fig. 2a, and a separate unbiased group of rats was used ($N$ = 15). In Fig. 2b, the reference voxels were placed in the SMT, and all voxels above the correlation threshold of 0.35 were plotted. The SMT exhibits correlation with M1/M2, CC, and ipsilateral S2. A strong correlation with contralateral SMT is clearly evident. In Fig. 2c, the six-reference voxels were selected from the center of the M1/M2. The cross cortical connection dominates this figure, with correlation to both contralateral and ipsilateral M1/M2, S1, and ipsilateral S2. Interestingly, in this case, the cortex to thalamus connection is quite diffuse, but some connection to the VL is evident that is not visible upon task activation (Fig. 2a). It is noted that the anatomical tract tracer studies have shown a direct connection between these areas (13). In Fig. 2d, reference voxels were chosen in the CP region, and the strongest correlation is between both sides of the CP.

The same analysis was performed on areas activated by visual stimulation. Figure 3a displays the task activation that occurs in a slice centered -5.36 mm from bregma after bilateral flashing at 1 Hz of blue LEDs into the rat's eyes. Areas with significant activation include bilateral LP, SC, and DLG, with minor changes in V1. Again, when the resting-state analysis is performed by placing six reference voxels in the center of the task-activated DLG (Fig. 3b), areas of correlation are displayed, including the opposite DLG and both sides of the SC and V1. As before, the same 15 unbiased rats were used in the resting-state analysis. Reference voxels were placed in V1 (Fig. 3c), and as in the motor system, the intracortical connections are extremely strong. However, correlation between V1 and DLG, LP, and SC exists with an expected bias toward the ipsilateral side.

Visual activation in another 1-mm slice centered -7.36 mm from bregma is exhibited in Fig. 3d. Strong positive BOLD activation occurs in the SC, LP, and V1 regions. The resting-state analysis was performed in this slice by placing the six reference voxels in the SC (Fig. 3e) and V1 (Fig. 3f). Interestingly, the resting network with the reference voxels in the SC (Fig. 3e) shows a bias toward extremely diffuse connections to the V2 and opposite SC and LP. Again as in the sensorimotor system, the intracortical connections overshadow all others when the reference voxels are in the V1 (Fig. 3f).

The sensorimotor and visual systems were also used for hypothesis-driven analysis. ROIs from Fig. 1a and b were drawn according to the rat brain atlas (3) and used for further analysis. All regions spanned multiple 1-mm slices, and an average filtered time course across the entire region was used in this investigation.

An RPCC matrix was generated for the sensorimotor system (Fig. 4). The matrix is symmetric about the main diagonal. The lower triangular part of the matrix displays a colored plot of the correlations between regions based on the color bar at the far right. The upper triangular part of the matrix contains the corresponding correlation coefficients. Along the main diagonal,

each regional time course is correlated with itself and therefore the entries have a correlation coefficient value of 1.0. Regions with a pairwise correlation above 0.35 are generally considered to be connected (1). A correlation of 0.35 corresponds to an equivalent *P* value after correction for temporal smoothness of 0.0016. The highest pairwise correlations are found in the intracortical and intrathalamic regions. There is also significant correlation from cortex to thalamus. All regions are strongly correlated to counterparts on the opposite side of the brain. The SC from the visual system is included in Fig. 4 as a control. We hypothesized that most of the regions in the visual system are not connected to the sensorimotor system and therefore should be uncorrelated. As expected, the SC has a low correlation (<0.30) to the regions within the sensorimotor network.

The RPCC matrix for the visual system was tabulated and is displayed in Fig. 5. The connections between V1 and V2 are the highest, which is because they are both cortical regions and are in close proximity. There is also very high correlation between regions within the thalamus (i.e., LP and DLG) to V1/V2 and also from SC to V1/V2. As in the sensorimotor system, left to right intraconnections within the same region are quite high. Interestingly, the correlations between the two distinct pathways in the visual system are quite low (for example, the pairwise correlations between LP and DLG (<0.42) and SC and DLG (<0.42)). Prior studies have shown that the two pathways to the cortex in Fig. 1a are distinct. The hippocampus (HIP) was chosen as a control because it was hypothesized to be uncorrelated to the visual system and also is located anatomically near many of the regions of the visual system. As shown in the matrix, the correlations between HIP and visual ROIs are below 0.35.

## DISCUSSION

The goal of this investigation was to demonstrate low-frequency physiological fluctuations in two distinct sensory systems in the rat brain. Direct stimulation of the nerves in the rat upper extremity with a surgically implanted electrode defined voxels used to define reference time courses in resting brain. This technique activates both the motor and sensory bundles located in the nerve and causes BOLD activation changes over the entire sensorimotor network in the brain. Forepaw stimulation by needle electrodes is the stimulation task most often used to demonstrate response in the S1 forelimb region (S1FL), and, in a few studies, in the thalamic and S2 regions (18). It is a more limited technique for determining reference voxels for resting-state analysis than the use of implanted electrodes.

The visual activation method used in this work to delineate resting-state networks is also new. Very few investigations have employed visual stimulation to induce BOLD signals in rodents (19,20). These studies have shown mainly subcortical activation to flash stimulation, but demonstration of cortical visual networks in the rat has been elusive. Our work here establishes the feasibility of activation of an extensive cortical visual system by flash excitation.

We found that both our RPCC matrices and resting-state correlation maps were congruent with not only our fMRI activation maps but also the known anatomy and physiology of the sensorimotor and visual systems. In particular, the primary pathways of the visual system in the rat proceed from the eye to the DLG to V1 as well as from SC to LP to V2 as previously established. These regions showed high correlations in the resting state. Likewise for the somatosensory system, the major components including thalamic centers; VP and PO and cortical representations; sensory S1/S2, and motor M1/M2 showed a high degree of correlation. In addition, correlations between homotopic regions across hemispheres suggest callosal connectivity.

The RPCC matrix was introduced in this paper as a means to visualize patterns of connectivity between brain regions. In Figs. 4 and 5, entries in the matrix are displayed in two ways:

colorized and numerical. Patterns are visualized in the color display, and precise values of correlation coefficients are determined for regional correlations of interest. The RPCC matrix was found to be helpful in comparing experimental results with connection flow-charts derived from the literature. See the Results section.

We also employed a novel anesthetic technique. The choice of anesthesia plays a critical role in the success of BOLD fMRI small-animal experiments. Most anesthetics have a strong impact on blood flow and metabolism of the brain and therefore can have a negative impact on the success of fMRI studies. Certain anesthetics are known to modulate BOLD resting-state physiological fluctuations in humans (21,22) and baseline BOLD signal in rats (23,24). Medetomidine hydrochloride (Domitor) is an injectable nonopioid synthetic alpha 2 adrenoreceptor agonist with a short half-life and dose-dependent sedative effects. There have been very few published fMRI studies utilizing medetomidine as the primary anesthetic in rodents (20,25).

Detection of resting-state BOLD fluctuations in animal models has been elusive. However, there have been a few early studies in rats, including the first abstract on the subject, which was written by the authors (26-30). In this work, we have established that spontaneous BOLD restingstate fluctuations are present also in rodents. The recent availability of commercial high-field MRI systems specifically designed for small-animal imaging was essential for detailed study of rat brain with voxel sizes in the range of tenths of millimeters. This resolution is sufficient to reveal entire networks during fMRI task activation in small animals.

As stated in our original discovery of physiological fluctuations in human fMRI (1), the neurophysiological basis for these fluctuations is not well understood. However, the cross-hemispheric nature of the correlations argues against the notion that highly correlated regions only share venous drainage networks. The issue of aliasing is different from rats to humans. When looking at the entire spectrum, only the cardiac signal is aliased in humans, whereas in rats both the cardiac and respiratory signals are aliased. In our original work in humans, the Fourier transform of the filtered time course showed peaks corresponding to the resting fluctuations around 0.01 Hz. As shown in Fig. 1d, the peaks corresponding to the resting fluctuations in rats show up at the higher frequency of 0.05 Hz.

Scatter plots formed from percent enhancement during activation and percent fluctuation during rest for all activated voxels were formed (data not shown), following the methodology introduced in Hyde et al. (31). Data were fit to the equation $y = ax + b$, and $R^2$ of the fit of the data to the equation were obtained. Values of $R^2$, a, and b, for the rat across eight animals were not significantly different from reported values for humans. The good fit of the model to the data supports the hypothesis that physiological fluctuations and response to task have the same biophysical basis. Consistency between rats and humans permits us to hypothesize that these values will be constant across mammalian species. It is notable that our anesthetic protocol seems to have no effect on these values.

We conclude that the regionally specific long-range correlations of spontaneous low-frequency physiological fluctuations in BOLD signals across somatosensory and visual sensory networks of the brain in the absence of external stimulation are present in rats and are congruent with the corresponding sensory networks activated by sensory-specific stimulation. Together with recent studies in primates, these results suggest that these phenomena are conserved across mammalian species.

## ACKNOWLEDGMENTS

We thank B. Douglas Ward, Hanbing Lu, Shi-Jiang Li, and Jay Neitz for their helpful comments and careful review of the manuscript. The authors would like to also thank Abbie Amadio and Karen Hyde for manuscript editing and figure preparation.

Grant sponsor: National Institutes of Health; Grant numbers: EB000215, EB000215-S1, GM56398; Grant sponsor: Counterdrug Technology Assessment Center, Office of National Drug Control Policy, White House; Grant number: DABK39-03-C-0058.

## REFERENCES

1. Biswal B, Yetkin FZ, Haughton VM, Hyde JS. Functional connectivity in the motor cortex of resting human brain using echo-planar MRI. Magn Reson Med 1995;34:537–541. [PubMed: 8524021]
2. Cho YR, Pawela CP, Li R, Kao D, Schulte ML, Runquist ML, Yan J-G, Matloub HS, Jaradeh SS, Hudetz AG, Hyde JS. Refining the sensory and motor ratunculus of the rat upper extremity using fMRI and direct nerve stimulation. Magn Reson Med 2007;58:901–909. [PubMed: 17969116]
3. Paxinos G, WC. The rat brain in stereotaxic coordinates. Elsevier Academic Press; New York: 2005.
4. Biswal BB, Van Kylen J, Hyde JS. Simultaneous assessment of flow and BOLD signals in resting-state functional connectivity maps. NMR Biomed 1997;10:165–170. [PubMed: 9430343]
5. Lowe MJ, Mock BJ, Sorenson JA. Functional connectivity in single and multislice echoplanar imaging using resting-state fluctuations. Neuroimage 1998;7:119–132. [PubMed: 9558644]
6. Xiong J, Parsons LM, Gao JH, Fox PT. Interregional connectivity to primary motor cortex revealed using MRI resting state images. Hum Brain Mapp 1999;8:151–156. [PubMed: 10524607]
7. Xiong J, Rao S, Gao JH, Woldorff M, Fox PT. Evaluation of hemispheric dominance for language using functional MRI: a comparison with positron emission tomography. Hum Brain Mapp 1998;6:42–58. [PubMed: 9673662]
8. Hampson M, Peterson BS, Skudlarski P, Gatenby JC, Gore JC. Detection of functional connectivity using temporal correlations in MR images. Hum Brain Mapp 2002;15:247–262. [PubMed: 11835612]
9. Hampson M, Olson IR, Leung HC, Skudlarski P, Gore JC. Changes in functional connectivity of human MT/V5 with visual motion input. Neuroreport 2004;15:1315–1319. [PubMed: 15167557]
10. Greicius MD, Krasnow B, Reiss AL, Menon V. Functional connectivity in the resting brain: a network analysis of the default mode hypothesis. Proc Natl Acad Sci USA 2003;100:253–258. [PubMed: 12506194]
11. Vincent JL, Patel GH, Fox MD, Snyder AZ, Baker JT, Van Essen DC, Zempel JM, Snyder LH, Corbetta M, Raichle ME. Intrinsic functional architecture in the anaesthetized monkey brain. Nature 2007;447:83–86. [PubMed: 17476267]
12. Kolb, B.; Tees, R., editors. The cerebral cortex of the rat. MIT Press; Cambridge, MA: 1990.
13. Paxinos, G. The rat nervous system. Academic Press; New York: 2004.
14. Jenkinson M, Bannister P, Brady M, Smith S. Improved optimization for the robust and accurate linear registration and motion correction of brain images. Neuroimage 2002;17:825–841. [PubMed: 12377157]
15. Cox RW, Hyde JS. Software tools for analysis and visualization of fMRI data. NMR Biomed 1997;10:171–178. [PubMed: 9430344]
16. Hamming, RW. Digital filters. Prentice Hall; Englewood Cliffs, NJ: 1983.
17. Jackson, JE. A user's guide to principal components. Wiley; New York: 1991.
18. Keilholz SD, Silva AC, Raman M, Merkle H, Koretsky AP. BOLD and CBV-weighted functional magnetic resonance imaging of the rat somatosensory system. Magn Reson Med 2006;55:316–324. [PubMed: 16372281]
19. Huang W, Plyka I, Li H, Eisenstein EM, Volkow ND, Springer CS Jr. Magnetic resonance imaging (MRI) detection of the murine brain response to light: temporal differentiation and negative functional MRI changes. Proc Natl Acad Sci USA 1996;93:6037–6042. [PubMed: 8650215]
20. Van Camp N, Verhoye M, De Zeeuw CI, Van der Linden A. Light stimulus frequency dependence of activity in the rat visual system as studied with high-resolution BOLD fMRI. J Neurophysiol 2006;95:3164–3170. [PubMed: 16394078]

21. Kiviniemi VJ, Haanpaa H, Kantola JH, Jauhiainen J, Vainionpaa V, Alahuhta S, Tervonen O. Midazolam sedation increases fluctuation and synchrony of the resting brain BOLD signal. Magn Reson Imag 2005;23:531–537.

22. Peltier SJ, Kerssens C, Hamann SB, Sebel PS, Byas-Smith M, Hu X. Functional connectivity changes with concentration of sevoflurane anesthesia. Neuroreport 2005;16:285–288. [PubMed: 15706237]

23. Kannurpatti SS, Biswal BB. Effect of anesthesia on CBF, MAP and fMRI-BOLD signal in response to apnea. Brain Res 2004;1011:141–147. [PubMed: 15157800]

24. Kannurpatti SS, Biswal BB, Hudetz AG. Baseline physiological state and the fMRI-BOLD signal response to apnea in anesthetized rats. NMR Biomed 2003;16:261–268. [PubMed: 14648886]

25. Weber R, Ramos-Cabrer P, Wiedermann D, van Camp N, Hoehn M. A fully noninvasive and robust experimental protocol for longitudinal fMRI studies in the rat. Neuroimage 2006;29:1303–1310. [PubMed: 16223588]

26. Kannurpatti, SS.; Biswal, BB.; Hudetz, AG. MAP reversibly modulates resting state fMRI low-frequency fluctuations in anesthetized rats; Proceedings of the 11th Annual Meeting of ISMRM; Toronto, Ontario, Canada. 2003; Abstract 1856

27. Kannurpatti SS, Biswal BB, Kim YR, Rosen BR. Spatio temporal characteristics of low frequency BOLD signal fluctuations in isoflurane anesthetized rat brain. Neuroimage. in press

28. Lu, H.; Gitajn, L.; Rea, W.; Stein, EA.; Yang, Y. Resting-state functional connectivity in rat brain; Proceedings of the 14th Annual Meeting of ISMRM; Seattle, WA, USA. 2006; Abstract 532

29. Williams, KA.; LaConte, SM.; Peltier, SJ.; Keilholz, SD. Investigating the influence of anesthesia on resting state connectivity in rats using multiple analysis techniques; Proceedings of the 15th Annual Meeting of ISMRM; Berlin, Germany. 2007; Abstract 2009

30. Zhao, F.; Zhao, T.; Zhou, L.; Wu, Q.; Yang, Z.; Hu, X. Resting-state functional connectivity and stimulation-induced neural activity in the cortex and sub-cortical structures of rat brain; Proceedings of the 15th Annual Meeting of ISMRM; Berlin, Germany. 2007; Abstract 1980

31. Hyde JS, Biswal BB, Jesmanowicz A. High-resolution fMRI using multislice partial k-space GR-EPI with cubic voxels. Magn Reson Med 2001;46:114. [PubMed: 11443717]

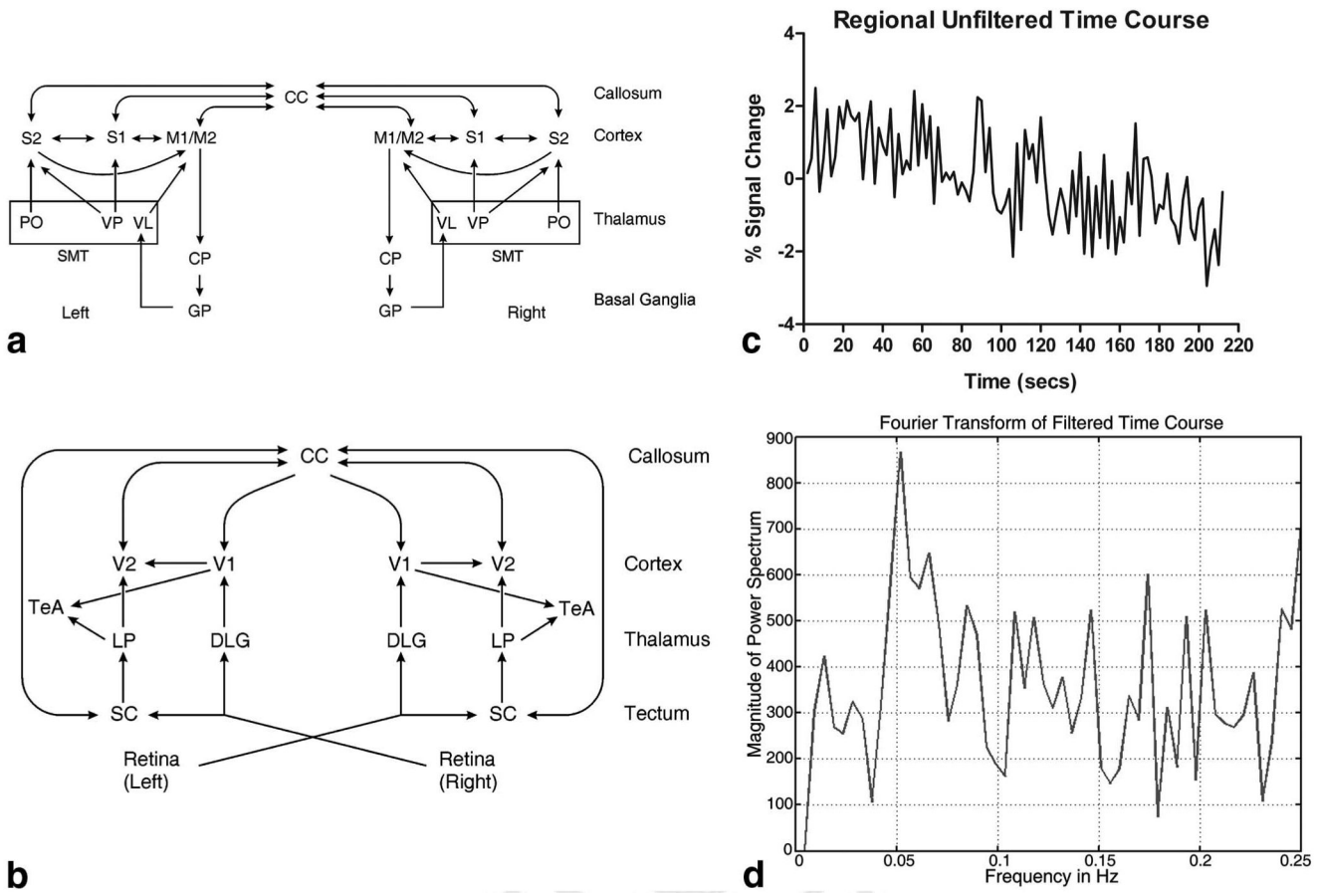


**FIG. 1.**

Simplified connection flowcharts of the rodent brain determined by prior work. **a:** Rodent motor/sensory system. **b:** Rodent visual system. System hierarchy moves from top to bottom. Arrows indicate primary information flow in the low to high hierarchy, although reciprocal connections are usually present. **c:** Percent BOLD signal change of a six-voxel reference region in the thalamus during a resting-state acquisition. This is indicative of a standard resting-state experiment. **d:** Filtered time course from (c) using a 0.1 Hz low-pass filter. Waveforms such as this are used in the analysis. See text for abbreviations.

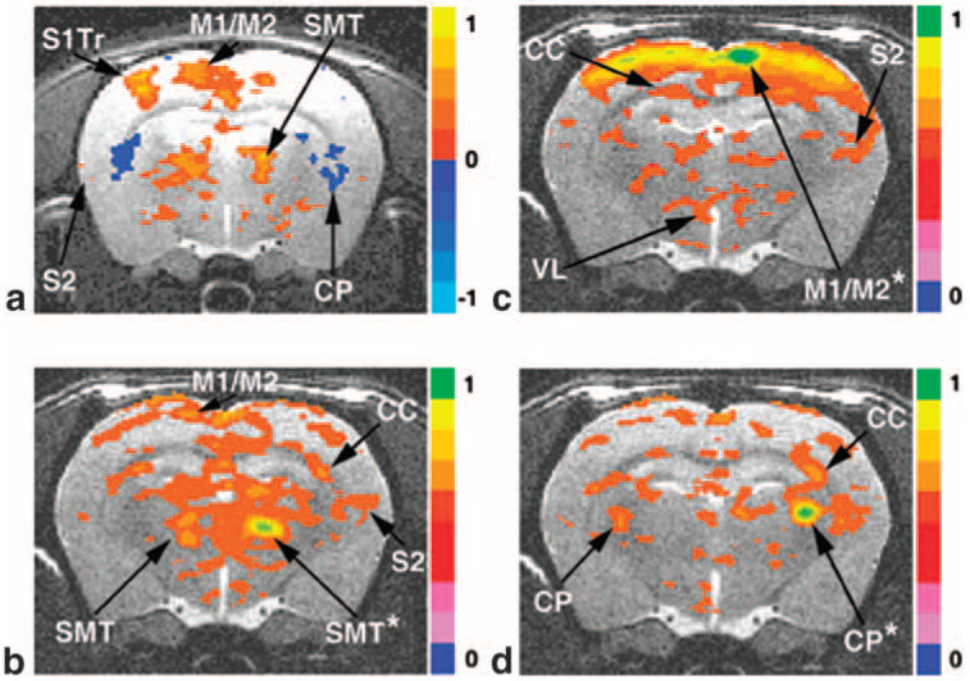


**FIG. 2.**

fMRI BOLD activation and resting-state connectivity maps of the rodent sensorimotor system. **a:** Direct radial nerve stimulation of the right upper forelimb; -2.90 mm from bregma. **b:** Reference voxels placed in the right SMT. **c:** Reference region in right M1/M2. **d:** Reference region placed in the right CP. (a) is an activation map with a voxel threshold at $P = 0.005$; (b), (c), and (d) are resting-state maps (0.35 threshold) from representative reference regions marked by asterisks. Results from 15 rats are averaged. See text for abbreviations.

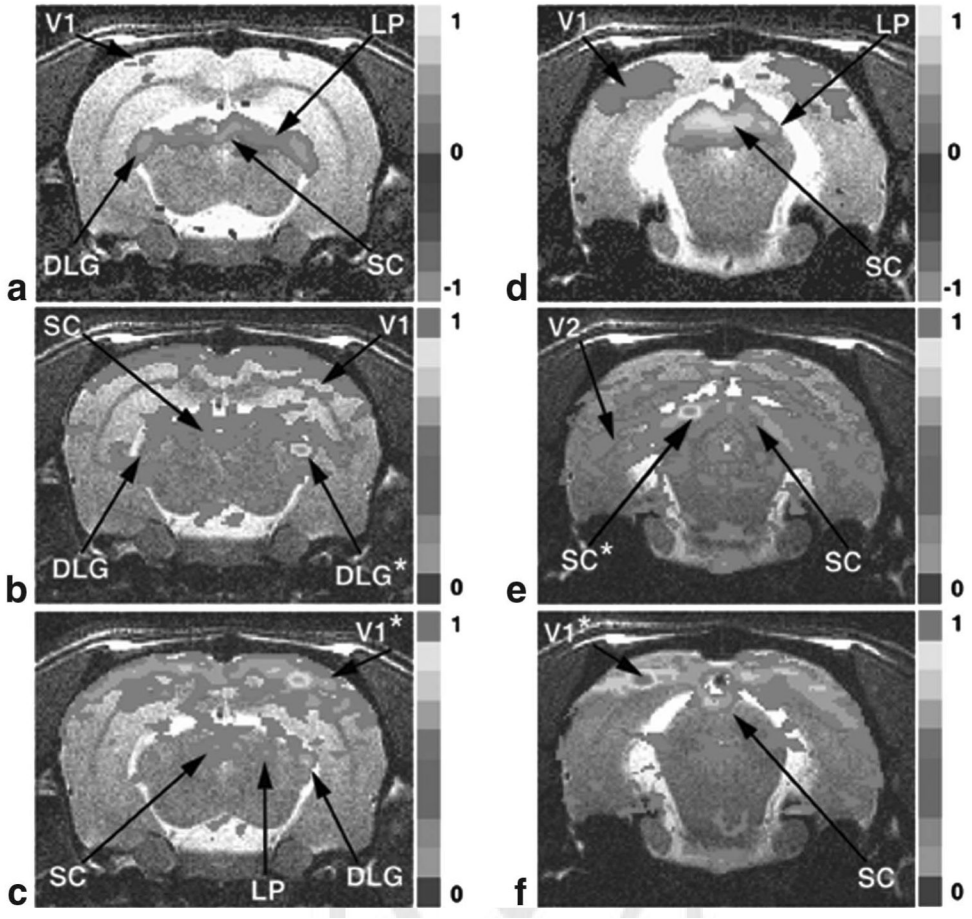


**FIG. 3.**

fMRI BOLD activation and resting-state connectivity maps of the rodent visual system. **a:** Bilateral blue LED flashing directly in the rodent eye; -5.40 mm from bregma. **b:** Reference voxels located in the right DLG. **c:** Reference voxels located in right V1. **d:** Bilateral blue LED activation; -7.32 mm from bregma. **e:** Reference voxels located in the left SC. **f:** Reference voxels in left V1. (a) and (d) are activation maps with a voxel threshold at $P = 0.005$. (b), (c), (e), and (f) are resting-state maps (0.35 threshold) from representative reference regions marked by asterisks. Results from 15 rats are averaged. See text for abbreviations. [Color figure can be viewed in the online issue, which is available at http://www.interscience.wiley.com.]

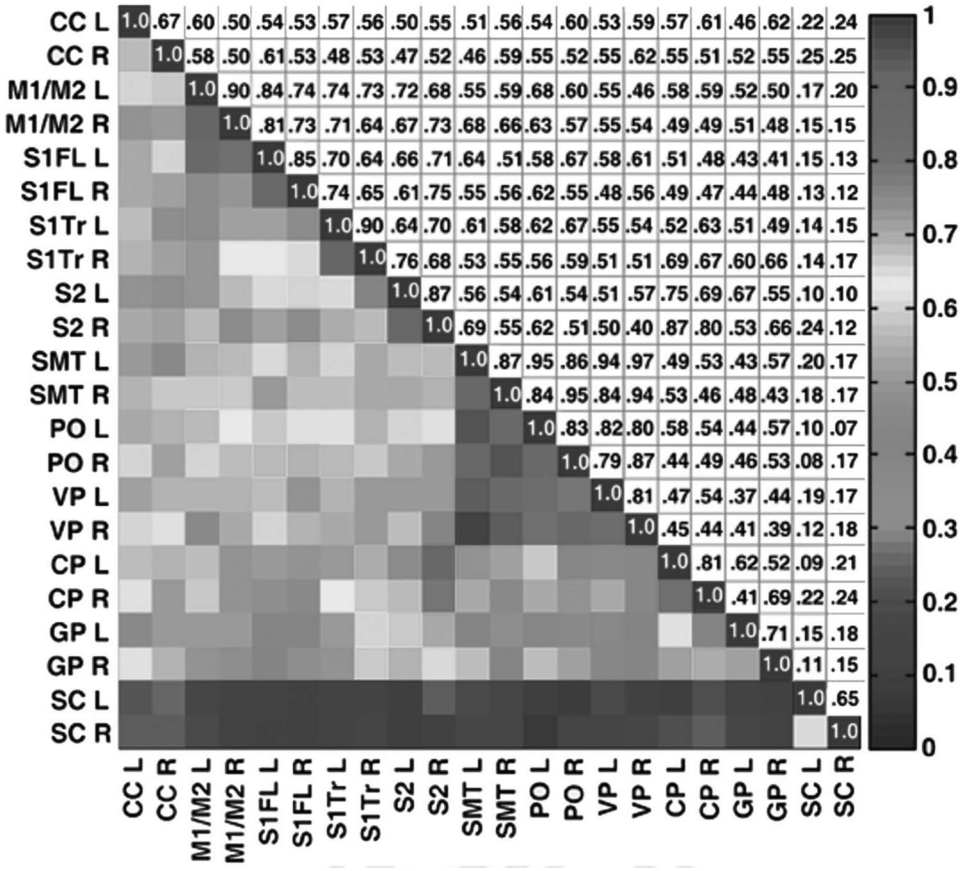


**FIG. 4.**

RPCC matrix of average resting-state BOLD time courses in the rat motor/sensory system. An average across 15 rats was used. Both the left and right side of each region were tabulated. The SC from the visual system was included as a control. The lower triangular part of the graph displays the coefficient values according to the color bar on the far right, and the upper triangular part (mirror image) of the graph tabulates the corresponding correlation coefficient values. Note the strongest correlations are intracortical and intrathalamic and the lowest correlations are in the control. See text for abbreviations. [Color figure can be viewed in the online issue, which is available at http://www.interscience.wiley.com.]

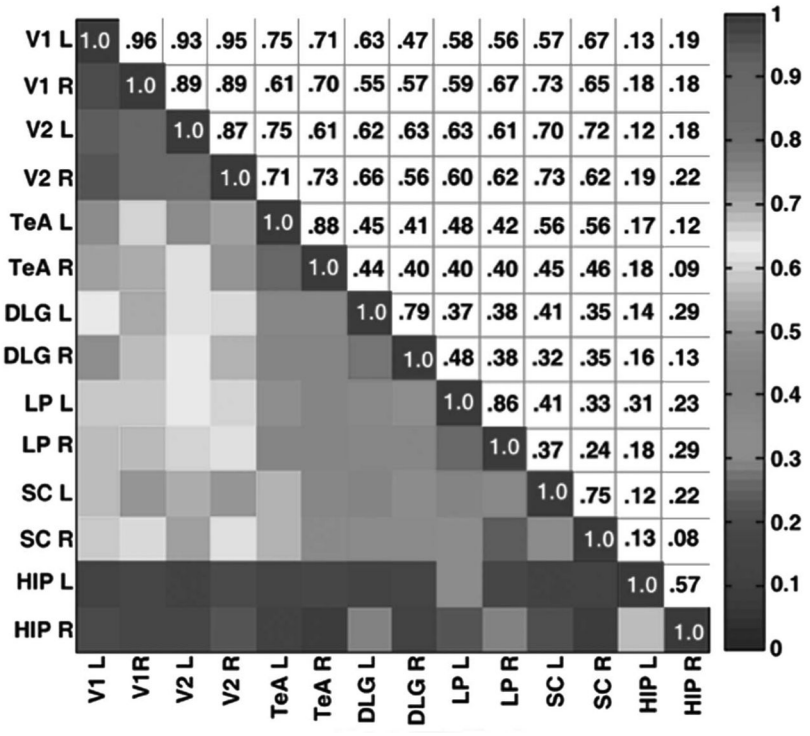


**FIG. 5.**

RPCC matrix of average resting-state time courses in the rat visual system. The average of 15 rats is used. The left and right sides of each region were tabulated. The lower triangular part of the graph displays the correlation coefficient values according to the color bar on the far right, and the mirror image lists the corresponding numerical values. Note the strongest correlations are within V1 and V2 and there is no correlation to the HIP control. See text for abbreviations. [Color figure can be viewed in the online issue, which is available at http://www.interscience.wiley.com.]